Effect of micro cooling channels on a hydrogen peroxide monopropellant microthruster performance

Jeongmoo Huh and Sejin Kwon
Department of Aerospace Engineering, Korea Advanced Institute of Science and Technology, 373-1 Guseong-dong, Yuseong-gu, Daejeon, 305-701, Republic of Korea

E-mail: trumpet@kaist.ac.kr

Abstract. In this paper, a hydrogen peroxide monopropellant microthrusters with and without regenerative micro cooling channels were fabricated and performance test results were compared to determine cooling effect of the regenerative micro cooling channels. Photosensitive glass was used as microfabrication material, which is cost-effective for MEMS fabrication process. Nine photosensitive glasses was integrated using UV and thermal bonding and composed the microthrusters. 90wt% hydrogen peroxide was used both as monopropellant and cooling fluid. For hydrogen peroxide decomposition, catalyst was fabricated and inserted into the microchamber. Platinum was used as the catalyst active material and γ-alumina was used as catalyst support. Experimental testing was conducted to determine effect of the cooling channels and the chamber pressure, temperature and surface temperature were measured. The performance test results showed that it was possible to relieve the thermal shock of the micro thruster structure by as much as 64% by adding regenerative micro cooling channels on both sides of the microthruster chamber. However, the chamber pressure and temperature decreased by regenerative cooling channels due to excessive cooling effects.

1. Introduction

For nanosatellites applications, many microthrusters has been developed using solid propellant propulsion. Solid propellant thruster has advantages of system simplicity, which is desirable for micro scale thruster operation, however, difficulties of throttling and re-ignition of the solid propellant thruster showed the limitation for nanosatellites attitude control, orbit compensation and orbit transfer. A monopropellant thruster is one alternative for nanosatellite applications, with system simplicity than that of bipropellant and possibility of throttling and re-ignition, which is difficult to function using solid propellant thruster. For these reasons, lots of microthruster was developed by monopropellant propulsion[1-3].

The microfabrication material with low thermal conductivity is desirable to conserve heat energy of the microthrustser, which has enhanced heat energy loss, due to large surface to volume ratio. Ceramics and glass are good fabrication material with low thermal conductivity and several previsou work shows the results of the microfabrication using these material. HTCC(high-temperature-co-fired ceramic) was used as an microfabrication material by Cheah et al.[4]. He found higher efficiency of the electric power consuming microthruster with HTCC than silicon, due to energy conservation effect of the fabrication material. LTCC(low-temperature co-fired ceramic) and glass were used also for microthrusters[3, 5]. Occasionally, however, brittle characteristics of the materials is a difficult challenge to overcome. Monopropellant microthruster was successfully fabricated using LTCC by Wu et al.[5], however, the crack occurred at the combustor wall and thrust level decreased. Glass was used by An[3] for micro reactor fabrication, and he found cracking of the micro chamber wall. These results showed the insufficient thermal strength of the ceramic and glass, which can be improved avoiding sudden temperature change and unevenly distributed thermal stress.

In this paper, a liquid microthruster with and without regenerative cooling channels were fabricated and to determine the effect of the cooling channels on the microthruster, which can be used for thermal shock handling. Experimental test was conducted and compared for the two microthrusters, and cooling channels effect on a liquid microthruster performance was studied.

2. Microthruster fabrication

The microthrusters were designed for 50mN class thrust generation, referring required microthruster thrust for nanosatellites operation[6]. Regeneratively cooled microthruster was designed and fabricated using nine glass wafers, and the components drawing is shown in figure 1. For similar heat capacity, uncooled microthruster was also designed and fabricated using nine glass wafers, and the drawing of the components is shown in figure 2. Using MEMS fabrication process, glass wafers were UV exposed using the pattern of designed microthruster profiles. Due to UV exposed parts of the glass is etched 20 times faster than unexposed parts by hydrofluoric acid, exposed glass can be selectively etched for the thruster profile. After polishing of the glass surfaces for thermal bonding, Nine glasses were integrated by both thermal bonding and UV bonding and composed the microthruster. Before all the wafers bonded, platinum/alumina catalyst was inserted into the catalyst with 100 mesh size sieve as catalyst holder, which catalyst was fabricated by the procedure of loading, calcination, and reduction. The integrated microthruster is shown in figure 3.

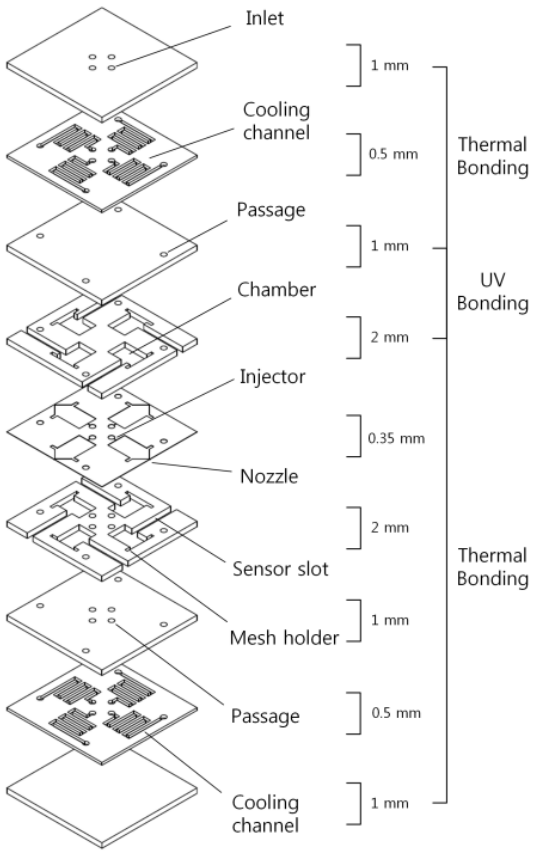

Figure 1. Regeneratively cooled microthruster components

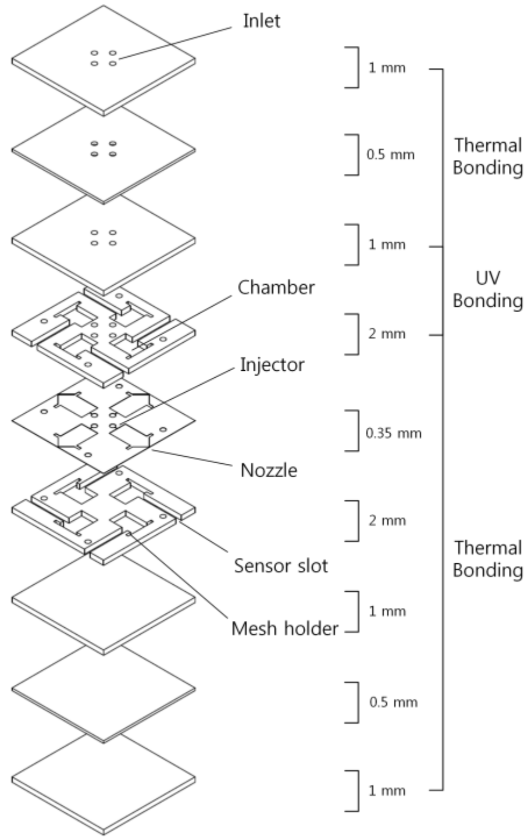

Figure 2. Uncooled microthruster components

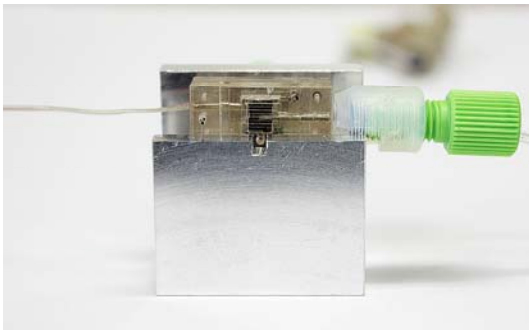

Figure 3. Integrated thruster installed at the thruster stand for performance test

3. Performance test and discussion

Experimental test was conducted with 90wt% hydrogen peroxide as a propellant, propellant feeding system and data acquisition device. Syringe pump and Teflon tubing composed propellant feeding system. The performance test results are shown in figure 4 and 5. Figure 4 shows the temperature differences for the chamber and surface of the microthruster. The chamber temperature was 323.0 ˚C for the cooled microthruster, and 582.6 ˚C for the uncooled microthruster. The surface temperature was 95.8 ˚C and 137.1 ˚C for cooled and uncooled microthruster, respectively. Figure 5 shows the chamber pressure differences between cooled and uncooled microthruster. The chamber pressure was 1.9 bar and 2.3 bar for the cooled and uncooled microthruster, respectively. Lower surface temperatures were desirable and it was intended for relaxation of thermal stresses stemming from abrupt temperature variations, but the lower chamber pressure and temperature are undesirable for thrust generation. The lower values for the pressure chamber might be explained by excessive effects from the cooling channels, which were experimentally determined for robustness during the wafer surface polishing process of the microfabrication procedure. The lower chamber temperature might cause a lower propellant decomposition efficiency by the catalyst, which varies exponentially depending on the temperature according to the Arrhenius equation.

Another factor we were interested in was the characteristic velocity. The characteristic velocity, also known as c*, is defined as:

$$c^* = P_c A_t / \dot{m} \tag{1}$$

where P_c is chamber pressure, A_t is nozzle throat area and $\dot{m}$ is mass flow rate. It may also be expressed in the following form for choked flow:

$$c^* = \frac{\sqrt{kRT_c}}{k[2/(k+1)]^{(k+1)/(2k-2)}} \tag{2}$$

where k is specific heat ratio, R is the gas constant, and T_c is chamber temperature. To find the degree of energy released from the propellant in a general rocket engine, c* efficiency is often used, which is the ratio of the actual value of c* derived from the equation (1) with the measured P_c to theoretical value of c* from the equation (2) using the estimated adiabatic temperature T_c. This is reasonable because the chamber temperature in the macroscale is very nearly the adiabatic temperature of the propellant. In the microscale, it is difficult to reach the adiabatic temperature due to excessive heat energy loss. Therefore, in this paper, as a denominator for the c* efficiency calculation, we used the actual c* determined from the measured chamber temperature, instead of the theoretical c* determined from the estimated chamber temperature. In other words, the ratio of c* derived from the equation (1) with the measured P_c to the c* from the equation (2) with the measured T_c was used. This describes how much chamber pressure was generated versus the temperature generated in the chamber. The performance results showed that the average maximum c* ratio at each pulse was 56.1% for the regeneratively cooled microthruster and 48.9% for the uncooled microthruster. This result may indicate that even though the temperature in the chamber was lower, the chamber pressure against the chamber temperature was relatively higher by as much as 7.2% with regenerative cooling channels than without. It may demonstrate the effectiveness of regenerative cooling even for non-optimized cooling channel design conditions.

The rise times for the pressure and temperatures were also estimated and were defined as the time for the values to reach 90% of their maximum from an initial state at each pulse. The results showed that it took an average of approximately 2.5 sec for the chamber pressure to reach 90% of its maximum for the regeneratively cooled microthruster and 3.0 sec for the uncooled microthruster. The rise time of the temperature was approximately 5.1 sec and 15.6 sec, respectively, for the chamber and the surface in the regeneratively cooled microthruster. In the uncooled microthruster, it was 3.5 sec and 7.5 sec, respectively, for the chamber and the surface. Despite the fact that the pressure rise time was lower and all of the maximum temperatures were lower, all of the temperature rise times were longer for the microthruster with the regenerative cooling channels than without. Therefore, lower thermal shock occurred with cooling channels. Using the definition of thermal shock as a temperature variation with respect to time, the maximum thermal shock of the microthruster chamber was approximately 63.9˚C/sec for the regeneratively cooled microthruster and 167.5˚C/sec for the uncooled microthruster. Additionally, the thermal shock on the microthruster surface was 6.2˚C/sec and 18.2˚C/sec with and without regenerative cooling channel, respectively. These results showed that the thermal shock was relieved by approximately 64% by adding regenerative cooling on the micro liquid monopropellant thruster. Figure 6 shows thermal shock the microthruster suffering at each pulse mode start, and approximately three times relieved thermal shock by regenerative cooling in the microthruser.

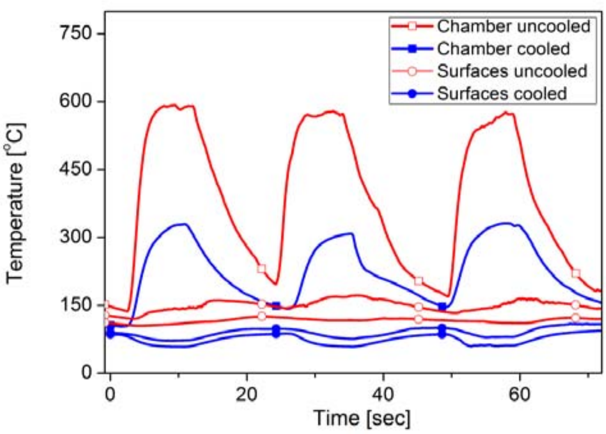

Figure 4. Temperature variations on three pulse operations

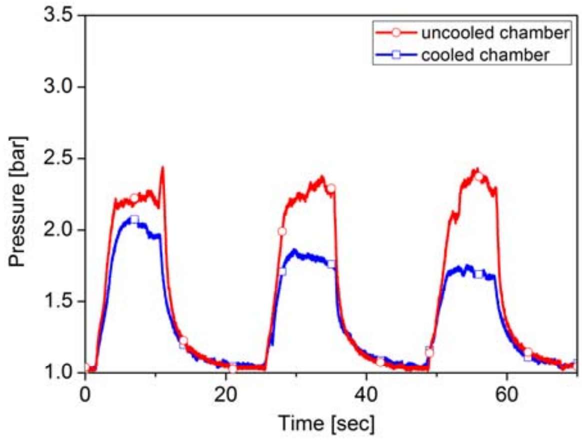

Figure 5. Chamber pressure variations on three pulse operations

Table 1. Summary of the microthruster experimental test results

Micro thruster test results	With channel	Without channel
Chamber presure+	1.9 bar	2.3 bar
Chamber temperature+	323.0 ˚C	582.6 ˚C
Surface temperature+	95.8 ˚C	137.1 ˚C
c* ratio#	56.1%	48.9%
Rising time of chamber pres	2.5 sec	3.0 sec
Rising time of chamber temp	5.1 sec	3.5 sec
Rising time of surface temp	15.6 sec	7.5 sec
Thermal shock in chamber	63.9 ˚C /sec	167.5 ˚C /sec
Thermal shock on surface	6.2 ˚C /sec	18.2 ˚C /sec

+ Average of the maximum values for each pulse
#Ratio of measured pressure c* to measured temperature c*

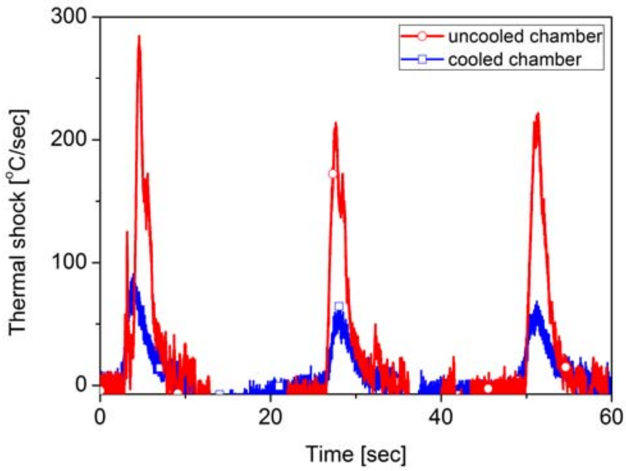

Figure 6. Thermal shocks of the cooled and uncooled monopropellant microthruster at each pulse start

4. Conclusion

Liquid monopropellant microthrusters with and without regenerative cooling channels have been fabricated and performance were compared for handling the thermal shock for microthrusters. Microthrusters with and without cooling channels were successfully fabricated and tested in this work. The performance results showed that despite the lower chamber and surface temperature in the regeneratively cooled microthruster, it took more time for the temperature to reach its maximum value, which reduced the chamber and surface temperatures variations with respect to time. Therefore, the thermal shock on the microthruster structure was relieved successfully, as much as 64% by adding regenerative cooling channels to the micro monopropellant thruster. Unexpectedly, the chamber pressure and temperature yielded poor results for the regenerative cooling channel, which may be accounted for by the excessive cooling effect of the channels and a lower propellant decomposition efficiency of the catalyst in the lower temperature condition. Additional work on cooling channel optimization to consider variations in the propellant decomposition efficiency of the catalyst as a function of temperature is expected to yield improved performance of the cooling channels.

Acknowledgment

This work was conducted at High-Speed Vehicle Research Center of KAIST with the support of Defense Acquisition Program Administration (DAPA) and Agency for Defense Development (ADD).

References

[1] Wu M H and Yetter R A 2009 Lab on a chip 9 910-6
[2] Huh J and Kwon S 2014 Journal of Micromechanics and Microengineering 24 9
[3] An S 2006 (Deajeon, South Korea: KAIST)
[4] Cheah K H and Low K S 2015 Journal of Micromechanics and Microengineering 25 10
[5] Wu M H and Lin P S 2010 Journal of Micromechanics and Microengineering 20 085026
[6] Janson S W, Helvajian H, Hansen W W and Lodmell L J 1999 In: The 2nd Int. Conf. on Integrated Micro Nanotechnology for Space Applications, (Pasadena, CA: The Aerospace Corporation)